Supplementary Information (SI) for Journal of Materials Chemistry B.

Maximising Efficacy in HER2-Positive Breast Cancer: Immunoliposomal Co-Delivery of miR155 Inhibitor and Paclitaxel for Targeted Therapy

Supplementary Table.1 The primer pairs used for different genes.

Gene Name	**Forward Primer**	**Reverse Primer**
GAPDH	CAGGAGGCATTGCTGATGAT	GAAGGCTGGGGCTCATTT
Bax	CCCGAGAGGTCTTTTTCCGAG	CCAGCCCATGATGGTTCTGAT
Bcl2	CTGCACCTGACGCCCTTCACC	CACATGACCCCACCGAACTCAAAGA
Caspase 3	CTCGGTCTGGTACAGATGTCGA	CATGGCTCAGAAGCACACAAAC
Caspase 9	GTGGACATTGGTTCTGGAGGAT	CGCAACTTCTCACAGTCGATG
APAF1	CACGTTCAAAGGTGGCTGAT	TGGTCAACTGCAAGGACCAT
P53	TCAGATCCTAGCGTCGAGCCC	GGGTGTGGAATCAACCCACAG
P21	AGGTGGACCTGGAGACTCTCAG	TCCTCTTGGAGAAGATCAGCCG

Supplementary Figure 1

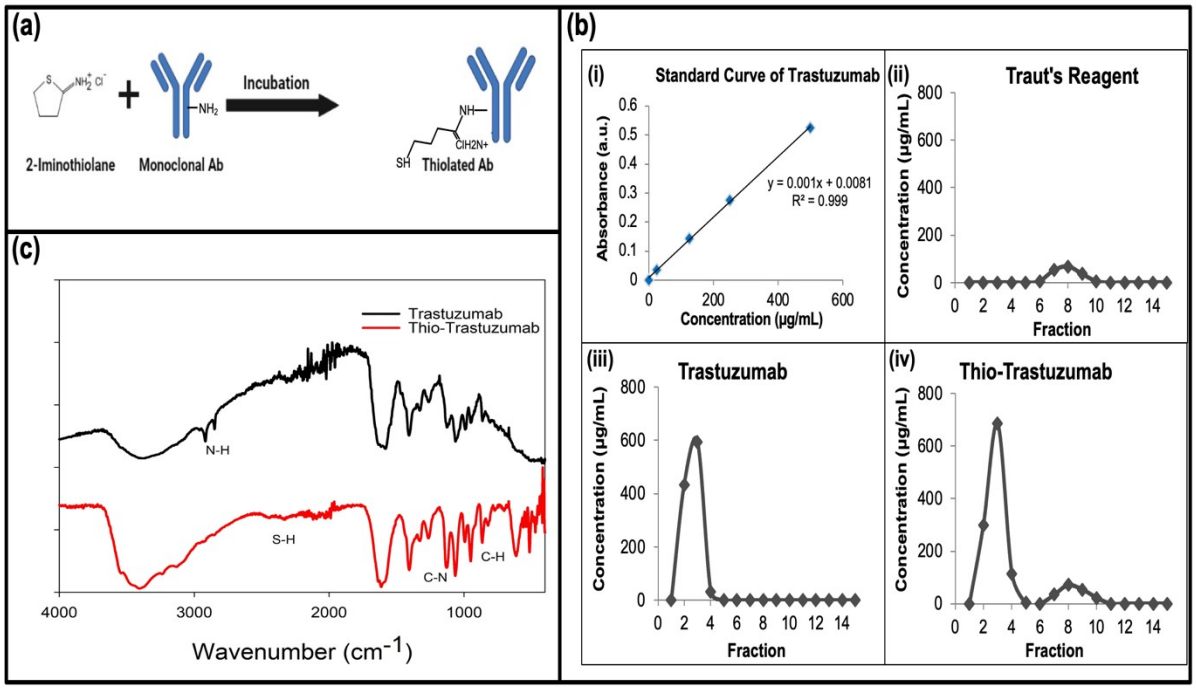

Thiolation Reaction of Monoclonal Antibody. (a) Schematic representation of the thiolation reaction of monoclonal antibody using Traut's reaction. (b) (i) Standard curve of trastuzumab antibody determined by BCA kit (ii) Fractions collected from PD-10 desalting column for trout's reagent. (iii) Trastuzumab antibody graph. (iv) Thiolated trastuzumab monoclonal antibody graph. The data presented in this panel demonstrates the successful purification of trastuzumab antibody and its thiolation using Traut's reaction. (c) FTIR spectrum compares the trastuzumab antibody and the thiolated trastuzumab, providing insights into the structural changes from thiolation.

Supplementary Figure 2

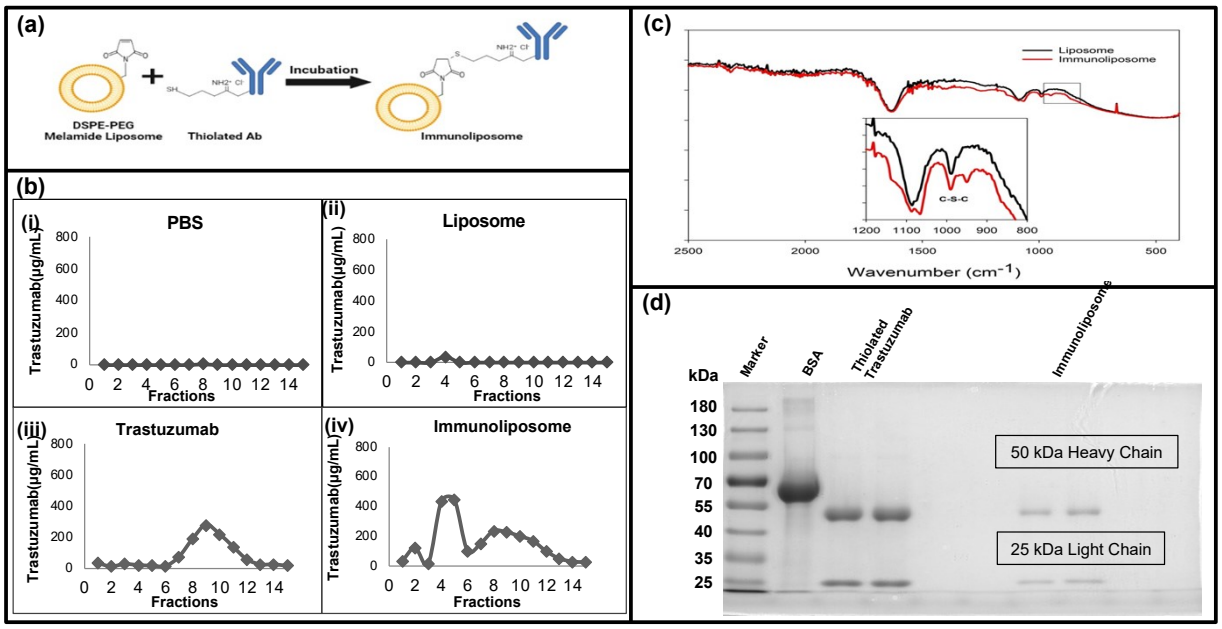

Conjugation of Thiolated Antibody on the Liposome. (a) Schematic representation of the conjugation reaction of the thiolated antibody with DSPE-PEG maleimide liposome. (b) Fractions were collected from the CL-4B desalting column for (i) PBS, (ii) Liposome, (iii) Trastuzumab antibody and (iv) Immunoliposome. The data presented in this panel demonstrates the successful purification of immunoliposomes. (c) FTIR spectrum compares the liposome and immunoliposome, providing insights into the formation of the c-s-c bond. (d) SDS-PAGE validating the attachment of antibody to the liposome.

Supplementary Figure 3

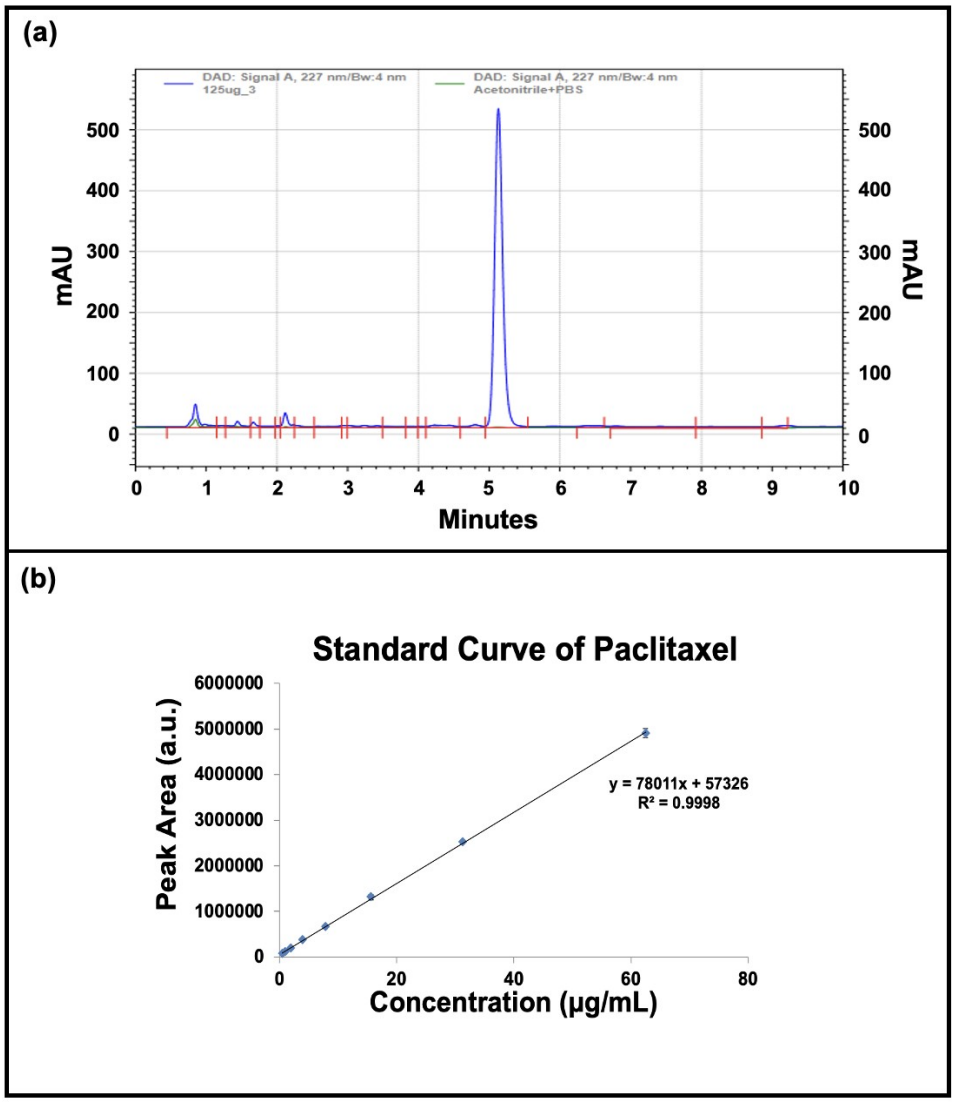

Characterization of paclitaxel (PXL) release. (a) HPLC chromatogram showing the elution profile of paclitaxel (PXL) and the ACN:PBS mixture. The peak corresponding to PXL confirms its presence and retention time in the ACN:PBS solution. (b) Standard plot for paclitaxel quantification using area under curve obtained from the HPLC chromatogram. The y-axis represents the peak area, while the x-axis denotes the PXL concentration.

Supplementary Figure 4

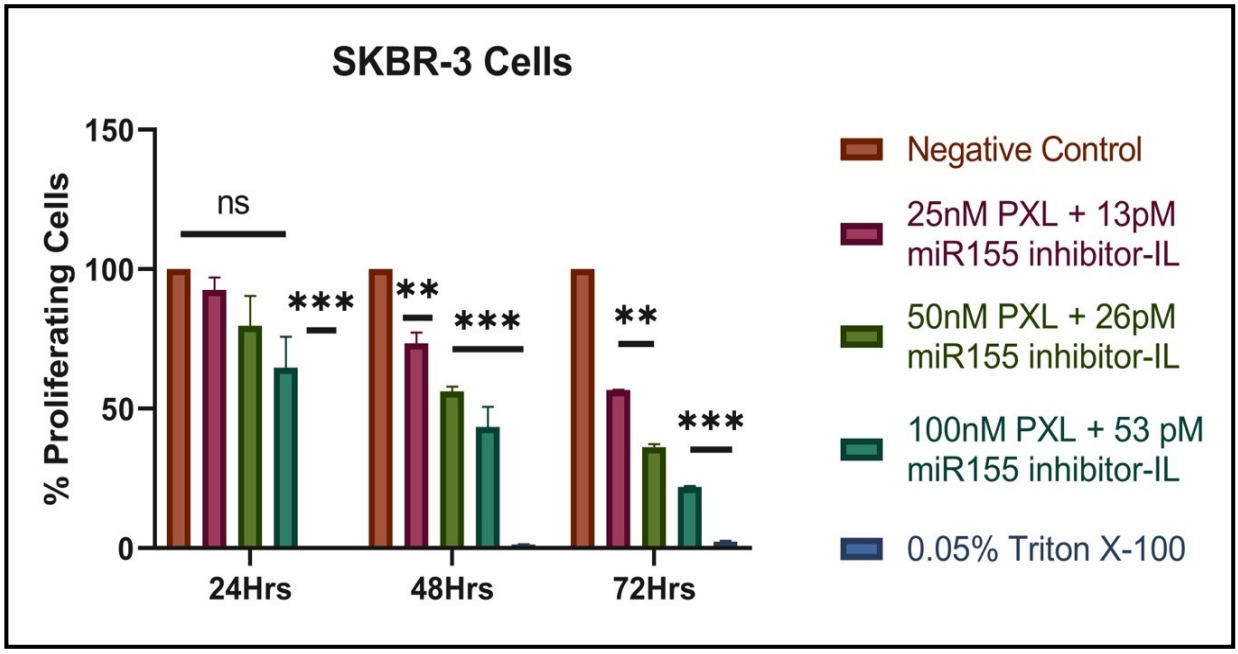

Effects of Immunoliposome Treatment on Cell Proliferation in SKBR-3 Cells. MTT assay results of SKBR-3 cells at different concentrations of immunoliposome. The graph indicates significant changes in cell proliferation at 48 and 72-hour time points.

Supplementary Figure 5

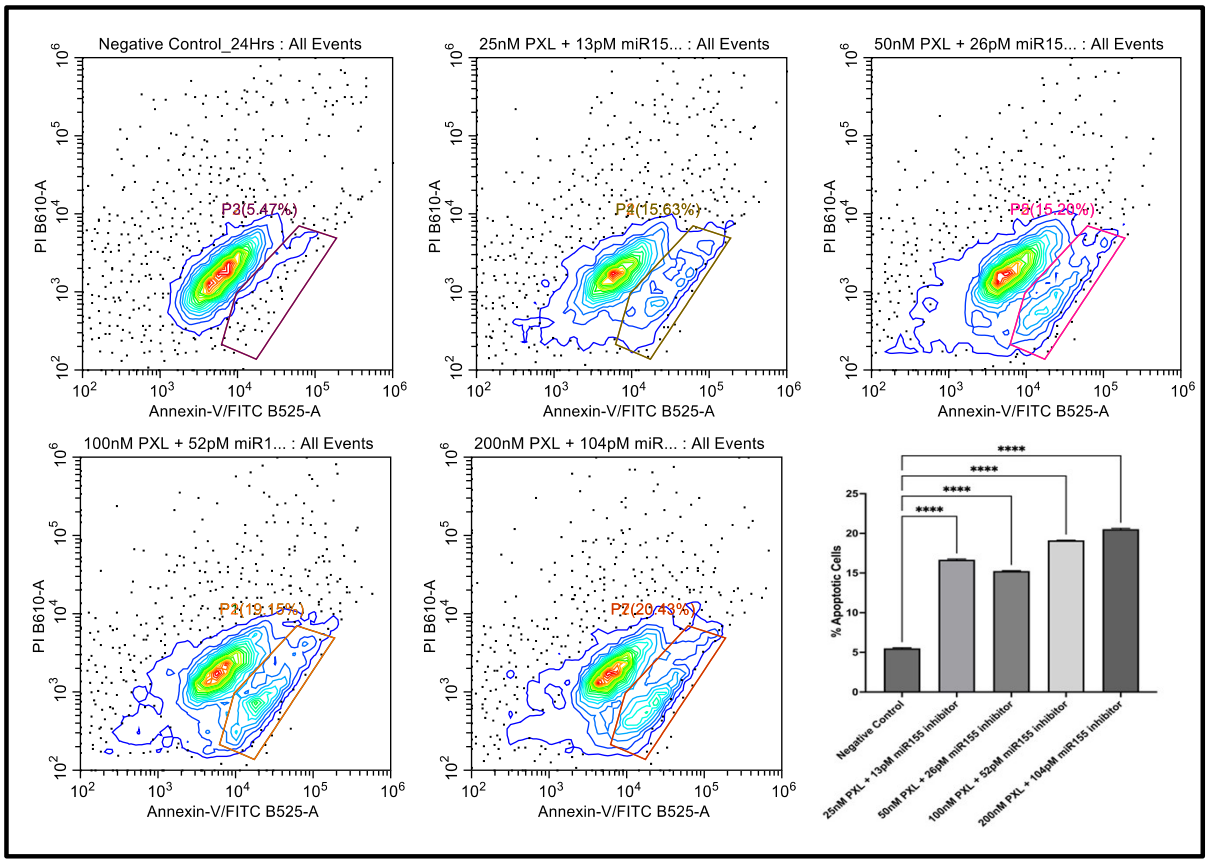

Annexin-V FITC Apoptosis Detection. Contour plots and bar graph indicating the apoptotic population in response to different concentrations of paclitaxel (PXL) and miR155-loaded immunoliposomes. The bar graph demonstrates the percentage of apoptotic cells for each treatment group after 24 hours of treatment. The y-axis represents the percentage of apoptotic cells, while the x-axis denotes the different treatment conditions. Statistical analysis reveals a significant increase in the apoptotic population for all concentrations of PXL and miR155-loaded immunoliposomes compared to the negative control group.

Supplementary Figure 6

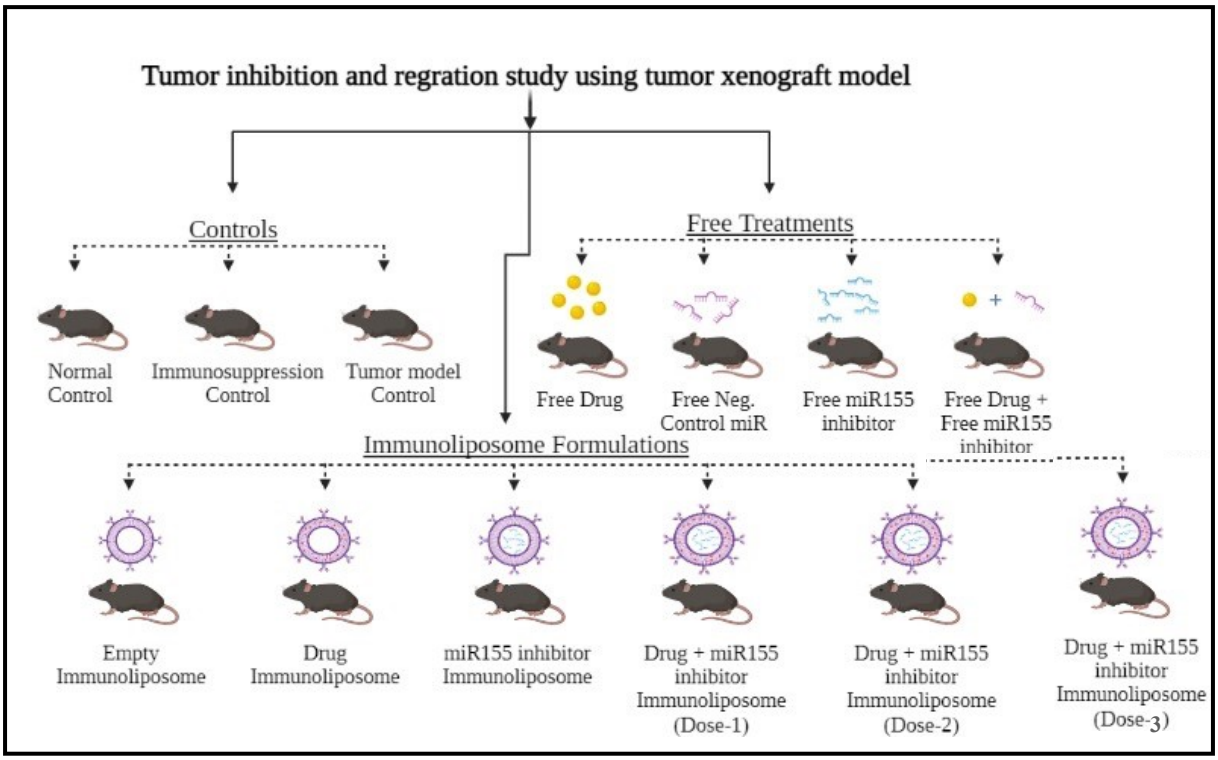

Schematic representing mice grouping and treatment.

Supplementary Figure 7

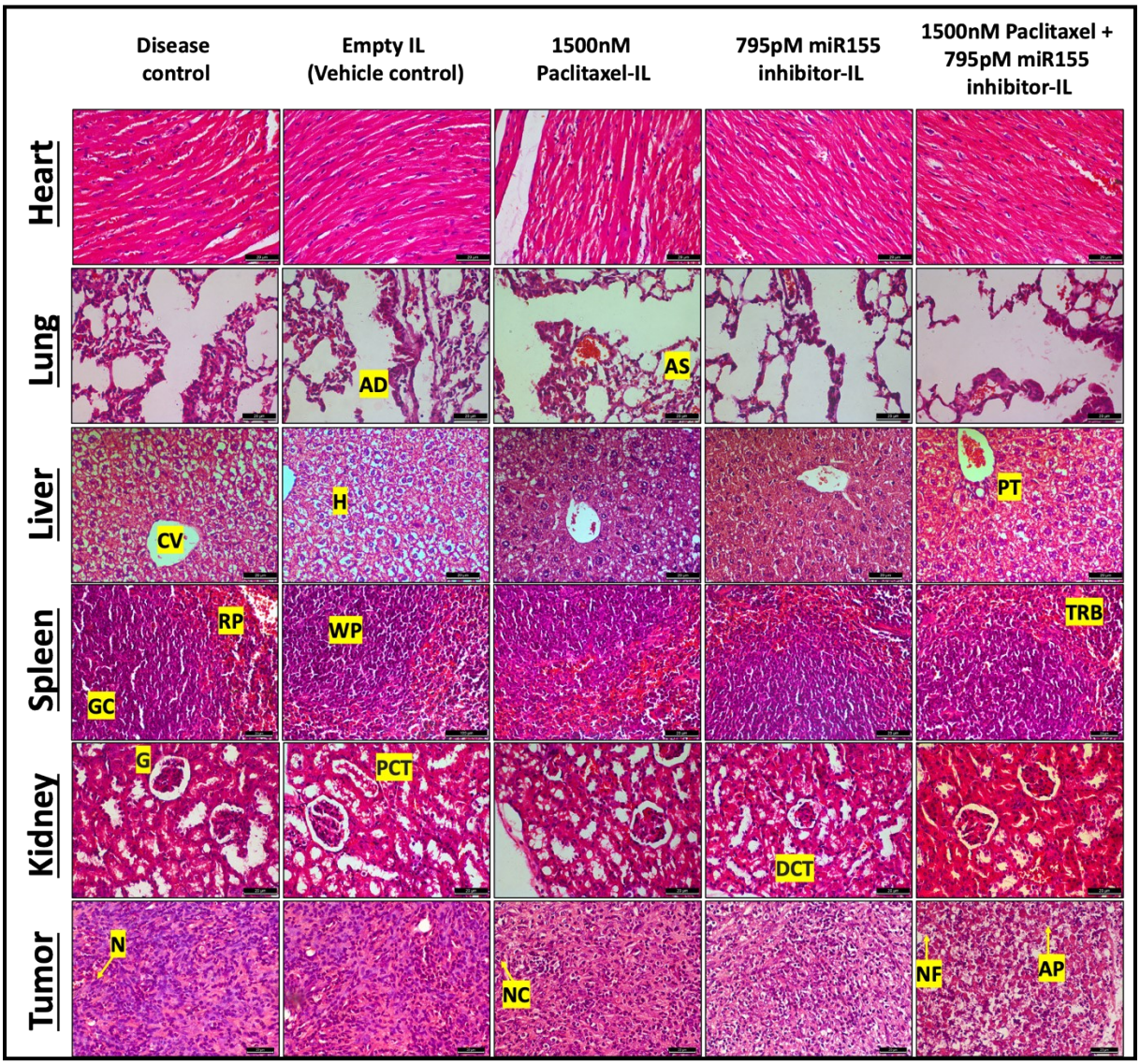

Comprehensive Histopathological Evaluation of Tissue Responses to Immunoliposome Therapy in HER-2 Positive Breast Cancer Xenograft Model Representative images of hematoxylin and eosin (H&E) stained tissue sections including heart, lung, liver, spleen, kidney, and tumor from mice treated with the formulated immunoliposomes. Images were captured at 40X magnification, revealing the histopathological architecture of each tissue type following treatment. **Abbreviations:** Alveolar Duct (AD), Alveolar Sac (AS), Central Vein (CV), Hepatocytes (H), Portal Triad (PT), Germinal Centre (GC), Red Pulp (RP), White Pulp (WP), Trabeculum (TRB), Glomerulus (G), Proximal Convoluted Tubules (PCT), Distal Convoluted Tubules (DCT), Nucleus(N), Nuclear condensation (NC), Nuclear Fragmentation (NF), and Apoptosis (AP).

Supplementary Figure 8

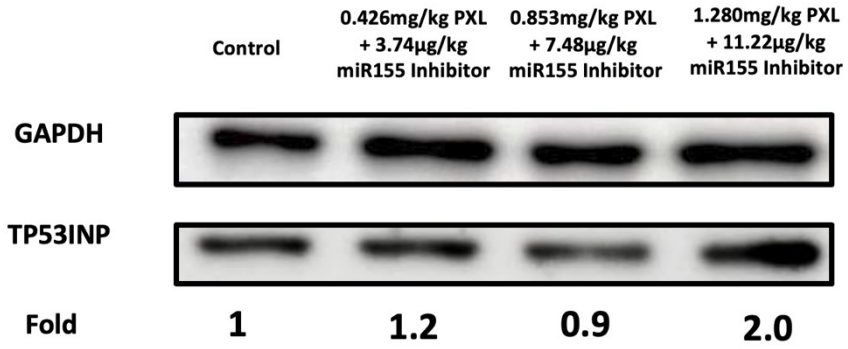

Western blot analysis of TP53INP1 protein expression in tumor samples. Fold change represented relative to control and normalized with housekeeping GAPDH. The most pronounced effect was seen at the highest concentration, showing a 2-fold increase in TP52INP expression.

Uncropped western blot images

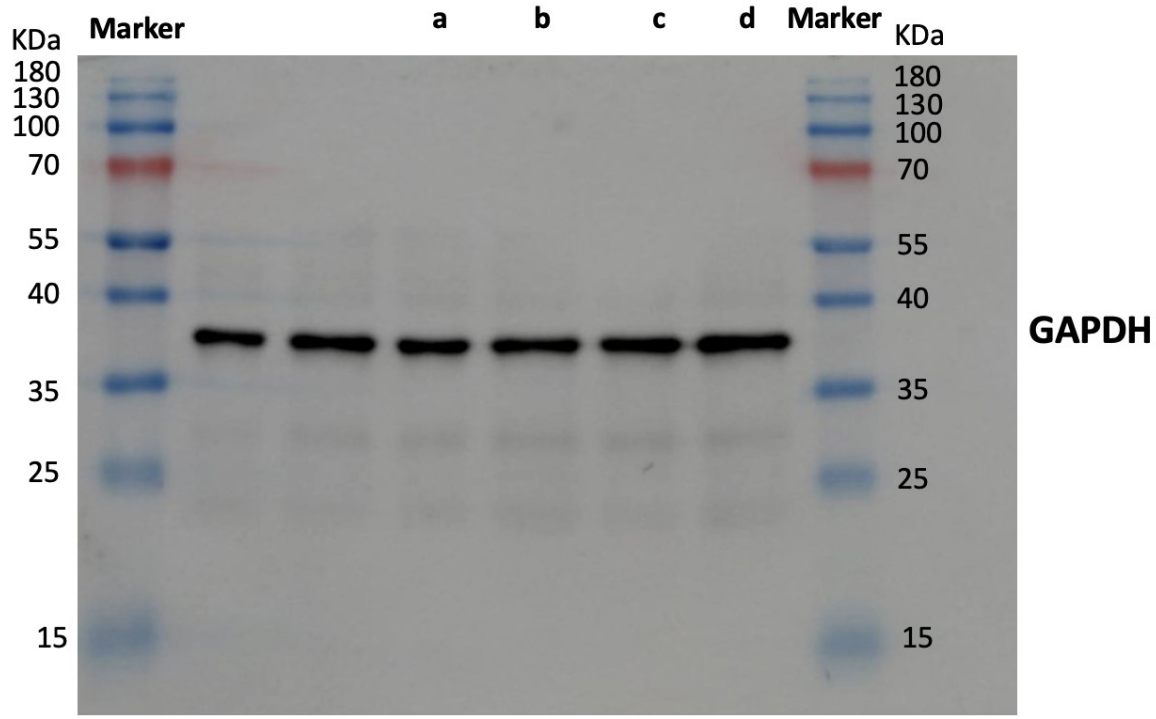

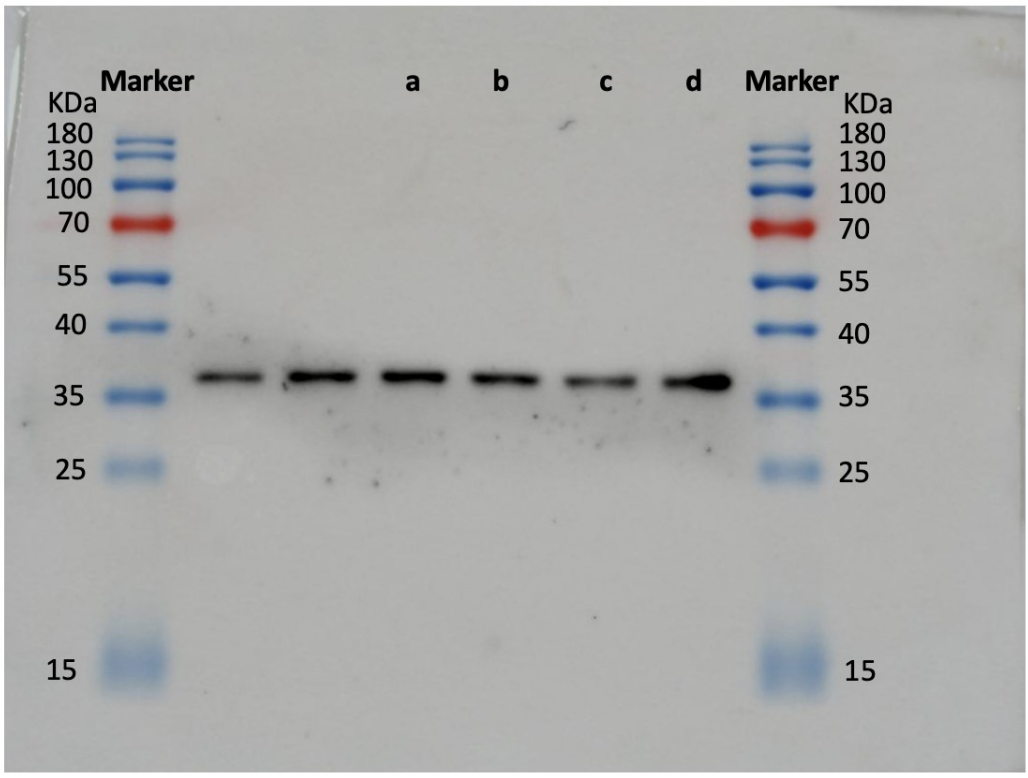

Lane a - Control (Disease Control)
Lane b - 0.426mg/kg PXL + 3.74ug/kg miR155 Inhibitor
Lane c - 0.853mg/kg PXL + 7.48ug/kg miR155 Inhibitor
Lane d - 1.280mg/kg PXL + 11.22ug/kg miR155 Inhibitor